Journal of Neurodevelopmental Cognition

Journal of Neurodevelopmental Cognition 6(1) (2025) 63-93 10.48308/jncog.2025.237954.1008

ISSN: 2645-565X

http://www.jncog.sbu.ac.ir

Nonlinear Brain Signal Processing to Model Learning and Memory Processes in Brain

Mohsen Najafi[1&2*], Mohammad Reza Arab[3], Faezeh Ebrahimi[1]

[1]*Faculty of Engineering, Arak University of Technology, Arak, Iran.*
[2]*Institute for Cognitive and Brain Sciences (ICBS), Shahid Beheshti University, Tehran, Iran.*
[3]*Intelligent Signal Processing and Cognitive Sciences Research Laboratory, Arak University of Technology, Arak, Iran.*

Abstract

Learning can be seen as a process of obtaining stable brain information that shows itself in thought, experiences, or behavior, and there is local memory for storing and retrieving information. In a nutshell, learning is a process that defines its output, memory. In this study, the behavior of learning and memory of ray was investigated along with dynamic analysis of signals. In this study, to create learning and memory processes, the Rey Auditory Verbal Learning Test (RAVLT) is used. In this study, 65 men and women with age range of 19-28 years and right hand have been used that 15 words in each stage are repeated for the subject and in each step, one needs to repeat it and repeat the EEG signals during these eight stages and before and after these stages in non-task relaxation conditions and 5 sub-frequency bands are analyzed. The statistical multivariate model demonstrates a correlation between behavioral learning rate (RAVLT) and three key parameters: the Hurst exponent, Higuchi fractal dimension, and approximate entropy of brain signals. The regression model highlights that the most significant predictor of learning and memory formation is the Higuchi fractal dimension of the signals, achieving an accuracy of 78.33% in predicting the learning rate. A second multivariate model, designed to estimate the behavioral learning rate based on the fractal dimensions of the sub-bands, achieves an accuracy of 73.27%. In this second model, the delta and theta frequency sub-bands exhibit the greatest effect size and the largest coefficients for predicting the learning rate. The study of this research shows that learning enhancement and synchronization process simultaneously reduces the entropy of approximation and the fractal analysis followed by Higuchi model which is the result of organizing the brain in information processing.

Keywords: Statistical Modeling, Learning and Memory Processes, Ray Auditory Verbal Learning Test (RAVLT), Higuchi Fractal Dimension

* Corresponding author

Email addresses: nadjafi43@gmail.com

Received: December 2024 *Accept: February 2025*

1. Introduction

Learning can be defined as a process of acquiring stable information in the brain, which manifests in thoughts, experiences, or behaviors, with memory serving as a repository for storing and retrieving this information. In summary, learning is a process whose outcome is defined as memory. This process, which leads to memory formation, begins with the intake of information. The information is then encoded in the brain, followed by consolidation, storage, and finally, retrieval in its last stage (Amina & Malikb, 2019).

These stages induce dynamic changes in the brain, which, due to the complexity of brain functions, pose significant challenges for researchers. Consequently, the brain is now often regarded as a complex, scale-free network. Moreover, this network exhibits fractal characteristics, making a static model insufficient for accurately representing brain behavior. This study aims to develop and propose a dynamic model tailored to the nature of learning, while also enabling the quantification of learning levels through brain signals. In conventional methods, learning is assessed behaviorally, typically through the completion of evaluation questionnaires (Dubinsky & Hamid, 2024). In this study, the Rey Auditory Verbal Learning Test (RAVLT) was employed alongside the dynamic analysis of signals. The RAVLT is a powerful and standardized method often used in neuropsychological sciences for comprehensive memory evaluation. It assesses a wide range of functions, including short-term auditory-verbal memory, learning rate, learning strategies, word recall at each stage of the test, learning curve registration, and the overall learning capacity of individuals. Furthermore, the RAVLT enables the evaluation of various memory abilities, such as immediate memory formation, delayed memory, forgetting rate, learning capacity, retrieval, and the interference effects of prior learning on new learning (proactive interference) as well as the impact of new learning on previous memory (retroactive interference). In this study, the Persian version of the RAVLT was utilized (Amina & Malikb, 2019; Arab et al., 2022).

Learning and memory are among the most fundamental mental processes, representing critical features of human intelligence. Most cognitive functions depend heavily on these two core processes (Arab et al., 2022). Additionally, learning and memory are deeply interconnected phenomena, allowing living organisms to acquire new knowledge about the world, retain it, and thereby shape their personality and relationships with the external environment(Amin & Malik, 2014; Antonis, 2023).

Some studies have attempted to define learning and memory as distinct processes. In these frameworks, the first stage involves acquiring and storing information in memory, the second focuses on maintaining and preserving this information over time, and the third stage involves retrieving and extracting the stored information when needed. Traditionally, the term "learning" has been associated with experimental operations emphasizing the first stage, whereas "memory" pertains to events occurring in the second and third Methods used to examine learning processes and memory formation so far have often relied on event-related potentials of the brain. These involve presenting task patterns to participants momentarily within a few hundred milliseconds on a monitor, ultimately leading to the formation of visual memories in the brain. In another study, non-semantic stimuli (e.g., music playback) were provided to participants, and their impact on signal behavior was analyze (Brem et al., 2013). One of the emerging approaches for estimating complexity and memory in time series is the use of the Hurst

exponent. Since long-term memory establishes dependencies between current and prior information, this parameter can be utilized to predict the memory capacity of brain signals (Baddeley, 2006; Brem et al., 2013).

Brain activity can be tracked using various neuroimaging techniques. Among these, electroencephalogram (EEG) provides excellent temporal resolution but poses significant challenges in understanding brain mechanisms due to the complex nature of brain functioning. This complexity extends to a scale-free behavior, as brain activities lack dominant temporal scales (Amina & Malikb, 2019; Antonis, 2023; Baddeley, 2006; Crowder, 2014), making EEG potentially more suitable for studying such mechanisms. EEG maps primarily illustrate cortical neural activity over time (Amin & Malik, 2014). EEG signals provide insights into brain states, adhere to a power-law distribution, and correspond to signal amplitudes across various frequencies. The power spectral density of EEG tends to decrease as the oscillatory frequency increases (Arab et al., 2022; Ceglarek et al., 2021; Ko et al., 2017).

One of the tools available for examining scale-free behavior is **fractal analysis**, which provides numerical descriptions of many natural phenomena (Amin & Malik, 2014; Feng et al., 2020; Wang et al., 2019). The concept of fractal patterns in EEG signals can manifest as variations in probability distribution functions, a slow decline in autocorrelation functions, or the presence of 1/f power spectra. Such statistical dependencies can be observed as either long-term and short-term correlations or as local and global similarities (Mitchell & Borasio, 2007). It has been shown that long-term correlations define memory within a time series. In this context, the **Hurst exponent** is widely used in fractal theory to measure long-term dependencies or the formation of memory in a time series (Basar, 2004; Birbaumer & Cohen, 2007; Kaufmann et al., 2014; Mitchell & Borasio, 2007; Ricci et al., 2012).

A cross-sectional analysis of EEG signals recorded during auditory stimulation has demonstrated that an increase in auditory memory formation is accompanied by an increase in memory formation in brain signals, as measured by the Hurst exponent (Basar, 2004). However, this finding was observed only during the sensory stage of learning and may not extend to long-term memory (LTM). This research aims to explore the mechanisms of LTM formation and models this process through an analysis of the Hurst exponent (Arab et al., 2022; Basar, 2004).

It has been shown that training can alter the structure and functions of the brain (Arab et al., 2022; Feng et al., 2020). These changes result from a learning process aimed at absorbing relevant information and shaping its representation. This phenomenon can be observed in brain activity across various levels of influence (Feng et al., 2020). For instance, changes in the power spectrum distribution of EEG signals and functional connectivity have been reported during semantic formation. Additionally, it has been demonstrated that the absolute and relative power of EEG frequency bands vary at different stages of learning (Feng et al., 2020). Other studies have proposed a generalized learning process based on newly self-organized memory models without evaluating neural responses, such as brain signals (Amin & Malik, 2014; Bongers et al., 2020). Additionally, event-related potentials (ERPs) have been used to assess working memory (Loftus & Loftus, 2019).

Modeling learning and its dynamics in the human brain has proven to be highly

challenging due to the complexity of neuronal interactions and diagnostic methods. Consequently, linear analyses have been largely ineffective in addressing this issue. To examine these complexities and the effects of learning and memory formation in the brain, nonlinear methods are employed (Ceglarek et al., 2021).

The examination of learning through brain signal processing in previous studies has been limited to the sensory stage (Amina & Malikb, 2019), during which information entering through auditory and visual senses is briefly stored in sensory memory without any processing. At this stage, the contents of brain signals are measured without influencing working memory (Amina & Malikb, 2019).

None of the previous studies have addressed the creation of long-term memory. The advantage of the learning assessment test used in this study compared to earlier research lies in the meaningful nature of the input information, which impacts semantic memory. Additionally, the test is not dependent on momentary events; rather, the information is presented continuously. Through repetition and practice over eight stages, it enhances the consolidation and encoding of information, enabling individuals to achieve mastery during recall. The outcome of this process facilitates the transfer of information into long-term memory. While previous research has primarily focused on short-term memory, this study introduces a novel model for the dynamic functioning of brain signals. Additionally, another model has been proposed to examine the role of frequency sub-bands during the learning stages.

EEG has been widely used to study brain behavior in various cognitive tasks such as learning, working memory, short-term and long-term memory (Maye et al., 2011), decision-making, intelligence tests (Davis et al., 2011), and mental problem-solving tasks (Davis et al., 2011; Wang et al., 2019). Changes in EEG measurements and features are closely associated with these cognitive activities (Wang et al., 2019). Spectral analysis of EEG and source estimation are employed to assess neural changes during different mental tasks (Michel & Brunet, 2019).

The effects of skill development resulting from the repetition of specific tasks in brain regions have also been studied using fMRI scanners (Kaufmann et al., 2014; Michel & Brunet, 2019). These results were examined through imaging under novice (processing) and expert (automatic) conditions. Another study investigated the level of visual learning in individuals with cognitive performance impairments. Additionally, in some articles, working memory performance has been analyzed using event-related signals in conjunction with visual tasks (Birbaumer & Cohen, 2007). The limitations of previous studies include:

1. Investigating learning in healthy individuals only in a sensory context, without considering semantic understanding.
2. The lack of analysis of learning dynamics in the brain resulting from memory formation.
3. The unclear quantification of memory content generated through learning.

The aim of this study is to statistically model the dynamics of learning using nonlinear analyses, leveraging a wide range of mathematical tools to achieve more comprehensive and accurate results. Here, we seek to take a broad perspective on the changes and organization of

continuous activity throughout the learning process and memory formation. To achieve this, we utilized the RAVLT framework for evaluating learning and memory processes. The RAVLT behavioral learning paradigm, which is capable of testing a wide range of learning and memory indicators, was employed alongside signal data, with the timing of their recording synchronized with behavioral stages. A multivariate statistical modeling approach was employed to determine the behavioral learning rate in RAVLT, using the Higuchi fractal dimension of EEG signals and the frequency sub-bands of brain signals.

The RAVLT evaluation framework, commonly used in rehabilitation centers, offers the ability to assess auditory-verbal learning and memory, analyze the learning rate, plot the learning curve at each test stage, and ultimately provide an overall index of learning ability (Skeel & Edwards, 2011).

In this study, participants underwent a word repetition test involving meaningful and independent words to assess their auditory memory. During the test phases, the participants' brain signals were recorded with relatively adequate spatial resolution. The number of words recalled by each participant was used to determine, based on a predefined formula, whether learning had occurred and to evaluate the auditory memory span for word learning using a curve analysis.

Standardized RAVLT assessments were conducted verbally, with a series of words presented to participants in five stages (Ricci et al., 2012). Brain signals were recorded during these stages as well as before the task, under resting conditions and with minimal external stimulation. The signals, following precise preprocessing and segmentation, were analyzed using nonlinear methods, including the Hurst exponent (for measuring memory capacity) and fractal dimension (for assessing complexity) across all learning stages. The relationship between these metrics and the number of words learned by each participant, as well as the correlation between changes in the Hurst exponent and fractal dimension, was examined. The statistical significance of these changes was determined through appropriate statistical analyses (Gneiting & Schlather, 2004).

The modeling and quantification of changes in brain signals or images, along with their results, primarily focus on the processes of encoding and recall, aligned with memory formation in subjects. The timing of information is typically limited to before and after learning, with minimal data available on events during the learning process.

In all techniques, brain potentials are recorded during momentary event-related tasks, such as n-back and Sternberg tasks. These tasks are generally devoid of semantic content and are primarily centered on working memory activities presented to the subjects (Geake, 2009).

In another part of this research, the dynamics of brain networks were analyzed by examining brain graphs generated from cognitive tasks and their parameters. These characteristics were compared with well-known models such as Watts–Strogatz (WS), Barabási–Albert (BA), and Erdős–Rényi (ER) (Basar, 2004; Bullmore & Bassett, 2011; Geake, 2009).

Structural changes resulting from motor skill learning represent another area of learning studies. This line of research has been facilitated by advancements in non-invasive thermal imaging technologies, such as diffusion tensor imaging (DTI), and the introduction of graph

theory. These approaches primarily enable the investigation of changes in white matter, gray matter, and brain plasticity in target groups within neural connectivity patterns. However, only a limited number of studies have focused on the topological features of brain networks related to motor skill learning, particularly free-form skills. Due to the complexity of processes involved in certain motor skills, such as learning to paint or sculpt, no research has yet been conducted in these areas (Bongers et al., 2020; Bullmore & Bassett, 2011). Learning and investigating the processes of memory formation, despite extensive research in recent years, remain among the critical and complex issues studied in functional cognitive research (Amina & Malikb, 2019).

One of the significant learning models closely aligned with the method of this study is the model proposed by Atkinson and Shiffrin. As illustrated in Figure (1), this model describes the processes within a multi-store memory structure. It assumes the existence of three distinct and independent types of memory, with information transferring between these stores in a linear sequence. The three primary storage locations include sensory memory, short-term memory (STM), and long-term memory (LTM).

The initial stage involves information processing, which begins when external stimuli are received by the senses. As depicted in Figure (1), the retention time for information in sensory memory ranges from a few milliseconds to a few seconds. Sensory memory exists for each sensory channel: **iconic memory** for visual stimuli, **echoic memory** for auditory stimuli, and **haptic memory** for tactile sensations. Sensory memory is a fundamental component of the perception process. The capacity of sensory memory is very large, though not unlimited like long-term memory. It is known that some memories last only a few seconds, while others endure for hours, days, months, or even years. Sensory stores are constantly receiving information; however, most of this information is disregarded and remains in sensory memory for only a very short duration. In sensory memory, information is derived from the five senses, such as vision (visual information), sound, and touch. Sensory memory has a high capacity but a brief duration, enabling it to encode information from each sense. Most of this information is lost due to decay (Amin & Malik, 2014; Amina & Malikb, 2019; Benedek & Fink, 2019).

Attention is the first step in remembering something. If an individual focuses their attention on one of the sensory stores, the data is transferred to short-term memory, also known as working memory. To elaborate, the common classification of memory divides it into the following types:

1. **Short-term memory (STM):** Includes memories that last for a few seconds or, at most, a few minutes unless they are consolidated into long-term memory.
2. **Medium-term memory:** Persists for days or weeks but is eventually lost.
3. **Long-term memory (LTM):** After consolidation, this type of memory can last for years or even a lifetime (Baars & Gage, 2010; Benedek & Fink, 2019; Loftus & Loftus, 2019).

After classifying memory based on this framework and defining the concepts of each type, we will now examine them in greater detail, focusing on the neuronal changes that occur within the nervous system during the formation of each type of memory.

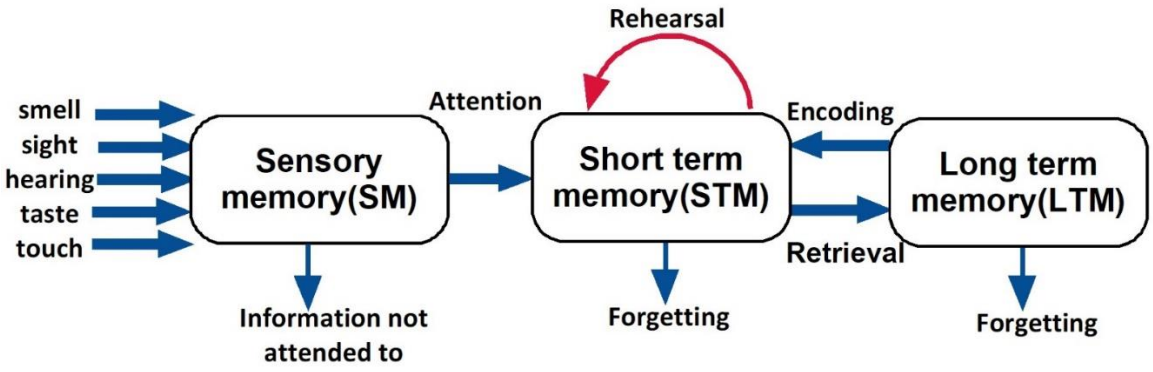

Figure *1* *The Atkinson and Shiffrin Multi-Store Memory Model.*

One of the most significant models of learning and memory interaction is the Atkinson and Shiffrin model. In this framework, information enters the sensory buffer through the five senses. Given the brief lifespan of this information, lasting only a few seconds, most of it is lost. However, if attention is directed toward or a specific stimulus is selected—typically visual or auditory—the information is transferred to short-term memory (STM) (Cowan, 2005).

Some researchers argue that this is essentially working memory, which actively processes and manipulates incoming information while linking it to previously stored data in the brain(Aben et al., 2012; Cowan, 2005). With repetition and practice, this information is transferred to long-term memory, where it can persist for days, years, or even a lifetime.

The memory process involves three main components: encoding of incoming information, consolidation and maintenance, and finally, retrieval. Repeated execution of these three stages increases the likelihood of information being retained in the brain, ultimately leading to the formation of **semantic memory** (memory for facts and concepts) and **episodic memory** (memory for personal experiences) (Arab et al., 2022).

The limitations of previous studies include the lack of exploration into semantic learning and memory formation in the brain, as well as the dynamic activities and impacts of created memory content. These changes have been validated in this study through behavioral auditory-verbal learning tests (RAVLT) conducted on participants.

In contrast to earlier studies, this research demonstrates that information passes through the sensory memory channel and, due to extensive rehearsal and repetition, undergoes significant encoding, consolidation, and retrieval. Ultimately, this process transforms the input into relatively stable auditory-verbal memory(Fard et al., 2016).

In this study, we utilized nonlinear fractal analysis to specifically calculate the Higuchi fractal dimension (HFD) of EEG signals and their frequency sub-bands (γ, β, α, θ, δ). The range of HFD values varied across the sub-bands, but the average HFD demonstrated a decreasing trend as memory levels increased in the cerebral cortex. This reduction in HFD indicates a decrease in randomness or complexity of the signals, a finding further confirmed by approximate entropy measurements (Arab et al., 2022).

Alongside changes in the fractal dimension of the sub-bands, the average relative power of these sub-bands was also analyzed. This measure showed an increasing trend across all frequency bands, except for the alpha band, which exhibited a decreasing trend. Additionally, the theta frequency band was identified as having the most active dynamics in enhancing the learning rate and memory formation, aligning with findings from previous studies.

The primary goal of these three stages is to assess the dynamics of learning and memory processes facilitated by auditory memory. This involves recording the subject's signals during learning and analyzing the impact of increased memory content using nonlinear analyses and the relative power of frequency sub-bands. Additionally, the study evaluates the recall of provided information through the RAVLT behavioral test and maps the fractal dimension distribution and changes in the relative power of frequency sub-bands associated with the learning stages.

2. Methods

2.1. Dataset

In this study, considering the temporal and spatial scope of the research, the statistical population consisted of male and female undergraduate students from the Electrical Engineering Faculty of Arak University of Technology. All participants were actively pursuing their bachelor's degrees at this institution and ranged in age from 19 to 28 years.

Due to the limited population size and the quasi-experimental nature of the study, a total of 65 subjects (43 males and 22 females) were selected as the statistical sample. Given that various factors can influence auditory-verbal memory performance, relevant information was collected from participants before conducting the interviews. This information included:

1- No history of medical conditions or any illnesses affecting cognitive health, including: chronic neurological disorders, cerebrovascular issues, brain tumors, strokes, head trauma, brain inflammation, Alzheimer's, epilepsy, Parkinson's disease, schizophrenia, AIDS, meningitis, intellectual disabilities, psychological or psychiatric issues, history of substance abuse or addiction to drugs and alcohol, use of psychiatric medications, sleep disorders, or hearing and speech impairments.

2- Monolingual, with proficiency in Persian as a native language.

It is important to mention that the test participants predominantly used their right hand for writing.

The level of anxiety, depression, and emotion in the study participants was measured using the DASS 42 questionnaire. The DASS 42 scale is capable of diagnosing and screening symptoms of anxiety, depression, and stress over the past week. This scale is intended for use with adults and has appropriate validity for application in research and diagnostic activities.

Although this test is capable of screening and diagnosing during adolescence, it is recommended for use with individuals over 15 years of age. Before recording brain signals, this questionnaire is completed as a self-assessment by the subject, and the score is determined based on the specified criteria. If the score from the 42 questions of the questionnaire, which

assess anxiety, depression, and stress, is lower than the normal and expected range, the individual will be excluded from the list of participants in the experiment (Benedek & Fink, 2019; Fard et al., 2016; Leahey).

The Rey Auditory Verbal Learning Test (RAVLT), adapted from the Persian version, was administered to participants. The examiner presented two distinct lists of 15 unrelated yet semantically meaningful words (Lists A and B). List A words were delivered at a rate of one word per second. Participants were instructed to recall as many words as possible from List A until they could no longer remember additional items. This procedure was repeated five times to assess the impact of repetition on stimulus encoding and learning capacity. Subsequently, List B was presented once under identical conditions. Immediately following the presentation of List B, without any intervening cues, participants were asked to recall words from List A. A 30-minute delay period was introduced, after which participants were again prompted to recall words from List A to evaluate long-term retention.

Table 1 *RAVLT test implementation steps related to one of the subjects*

Recall of Words from the First List		Recall of Words from the Second List		Recall of Words from the First List						No
Stage 8	Stage 7	Stage 6	Second List	Stage 5	Stage 4	Stage 3	Stage 2	Stage 1	First List	
√	√	√	book	√	√	√	√	√	bowl	1
√	√	√	flower	√	√	√	√	√	dawn	2
√	√	√	train	√	√	√	√	√	judge	3
√	√	√	carpet	√	√	√	√		gift	4
√	√	√	forest	√	√	√			insect	5
√	√	√	song	√	√	√	√		plain	۶
√	√		salt	√		√	√		country	۷
√	√		finger	√	√	√			pool	۸
√	√	√	apple	√	√	√	√	√	grain	۹
√	√	√	heater	√	√	√	√		sheep	۱۰
√			button	√	√	√			food	۱۱
√	√		tree	√	√	√	√	√	coat	۱۲
√	√	√	key	√	√				bottle	۱۳
√	√	√	camel	√	√	√	√	√	beach	۱۴

√	√	√	gold	√	√	√	√	√	chair	۱۵
15	14	11		15	14	14	11	7	Number of Words Recalled	

In the RAVLT learning and memory consolidation test, if the result of the following equation (1) yields a positive LOT value, it indicates high activity and dynamics of working memory. In this case, due to the repetition of words, information is transferred to long-term memory (LTM) according to the Atkinson and Shiffrin multi-store model, due to encoding and recall processes. As a result, the individual will retain the ability to recall words for some time after the test(Daryadar & Raghibi, 2015).

$$\mathrm{LOT} = \mathrm{LT} - (5 * \mathrm{WS}_1) \qquad (1)$$

WS_1: Number of words recalled in the first stage of the test
LT : Total number of words recalled across all 5 stages of the test
LOT : Total learning rate

As observed in these stages of word presentation for the participant, in the sixth stage (trial 6), list "B" with 15 new words is presented to the participant. The effects of previous memory on the participant cause interference and a decline in the upward learning trend, which is why this stage is referred to as the interference stage. The curve of the recalled words one of the subjects is shown in Figure (2).

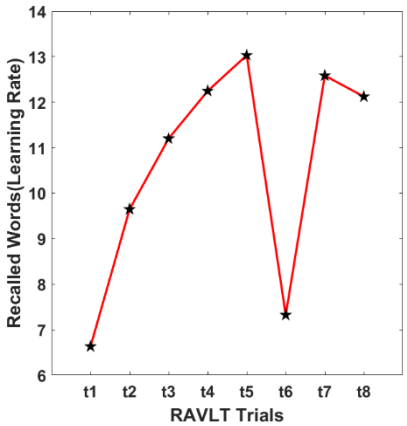

Figure 2 *Graph of the number of words recalled by a participant during the stages of the RAVLT.*

2.2. EEG Signal Recording

EEG signals were recorded from 32 channels based on the 10-20 system, with channel 32 connected to the lower right eye for recording Electro Ocular Ophatalmography (EOG) signals. Efforts were made to ensure the recording environment was free of external stimuli (e.g., sound, 50 Hz urban noise) that could degrade signal quality. The maximum impedance between the scalp and the recording electrodes was maintained below 10k Ω.

The EXG devices used, manufactured by the knowledge-based company Parto Danesh, feature a 1 kHz sampling frequency and a 24-bit analog-to-digital converter. These devices are capable of recording a variety of bio-signals (EEG, ECG, EOG, EMG, ECoG, etc.). The reference and ground electrodes were placed on the mastoid bone behind the ears to minimize artifacts.

EEG signals from participants were recorded in 10 stages, with each stage lasting 100 seconds. These stages included:

1. Resting state before the AVLT test (rest1).
2. Eight stages during the AVLT test (trial1...trial8).
3. Resting state after the AVLT test (rest2).

The workflow of these stages is illustrated in the block diagram in Figure (3).

Given the influence of anxiety, stress, and emotional states on learning and memory formation, all subjects were evaluated using the DASS42 (Depression, Anxiety, and Stress Scale (Sulak & Koklu, 2024). Only those who achieved a normal threshold score on this test were eligible to proceed with the auditory-verbal learning test (RAVLT).

This test, through the repetition and rehearsal of input information as outlined in the Atkinson and Shiffrin model, also facilitates the transfer of information to medium-term memory (Alsaeed, 2017; Sulak & Koklu, 2024).

a) Pre-learning (rest1) and post-learning (rest2) stages: Signals were recorded under closed-eye and open-eye conditions for 3 minutes each. These stages were conducted before and after the memory and learning tasks, which involved the execution of the RAVLT.

b) During the RAVLT execution: EEG signals were recorded during 8 stages (trial1...trial8) based on the relevant instructions, with each recording lasting 120 seconds.

This procedure encompasses the pre-test resting stage (rest1), the 8 learning stages during the behavioral RAVLT test, and the post-test resting stage (rest2). A graphical summary of these study stages is illustrated in Figure (3).

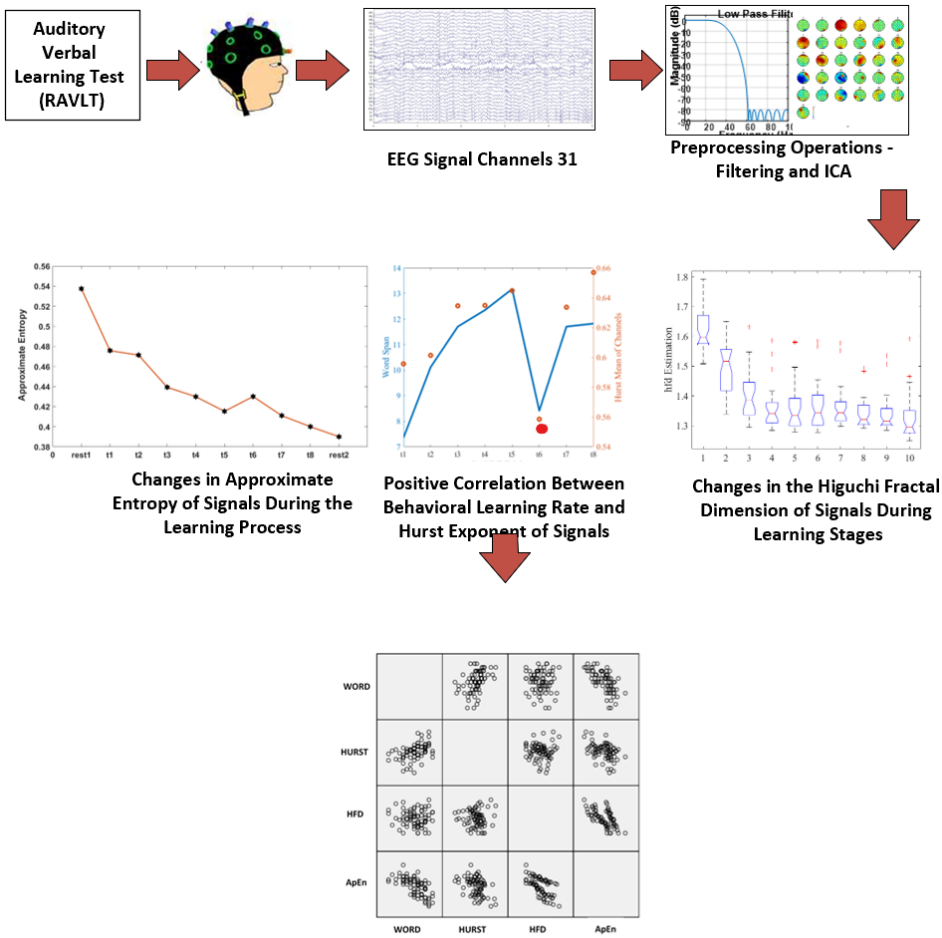

Figure 3 Graphical Summary of the Study Stages

2.3. EEG Signal Preprocessing Steps

1. Bandpass Filtering: A 4th-order Butterworth bandpass filter was applied to all signals, with a frequency range of 1–48 Hz.

2. Artifact Removal Using ICA: The EEGLAB toolbox was used to implement the Infomax Independent Component Analysis (ICA) algorithm to eliminate complex artifacts such as ocular and muscular artifacts.

3. Channel Removal and Interpolation: Channels that could not be artifact-corrected using the above method were removed. Although the number of such channels was very limited, channels with a statistical kurtosis value exceeding 5 were flagged as bad and excluded. Subsequently, the removed channels were reconstructed using spherical interpolation. The affected channel c(t) was recalculated based on neighboring channels c1 and c2 using Equation (2).

$$c(t) = \frac{\sin(1-t)}{sin\theta} c_1 + \frac{\sin(t)\theta}{sin\theta} c_2 \qquad \cos\theta = c_1 . c_2 \qquad (2)$$

4. The first 60 seconds of the signals, equivalent to 60,000 samples, corresponding to the time of the RAVLT test execution, were selected. The initial 15 seconds of this signal relate to

information input, encoding, and stabilization through auditory and verbal memory, while the remaining time corresponds to the recall of words by the participant.

5. To extract sub-frequency bands, the wavelet packet algorithm was employed in 7 decomposition stages, as illustrated in Figure (4). Due to the smoothing characteristics of the db4 wavelet and its extensive use in processing vital signals, this wavelet was applied in this study (Alsaeed, 2017; Brown et al., 1994; Miller, 2020). The coefficients obtained from the 7-level decomposition through the wavelet packet algorithm are structured as follows:

- For the beta band (12–32 Hz), two wavelet packet coefficients, N (5,1) and N (7,3), are required for reconstruction.
- For all other sub-bands, a single wavelet packet coefficient suffices for reconstruction.
- These coefficients were also employed during the calculation of the spectral energy of the sub-bands for signal processing.

Figure 4 Stages of EEG decomposition using the wavelet packet method for extracting the sub-frequency bands Delta, Theta, Alpha, Beta, and Gamma.

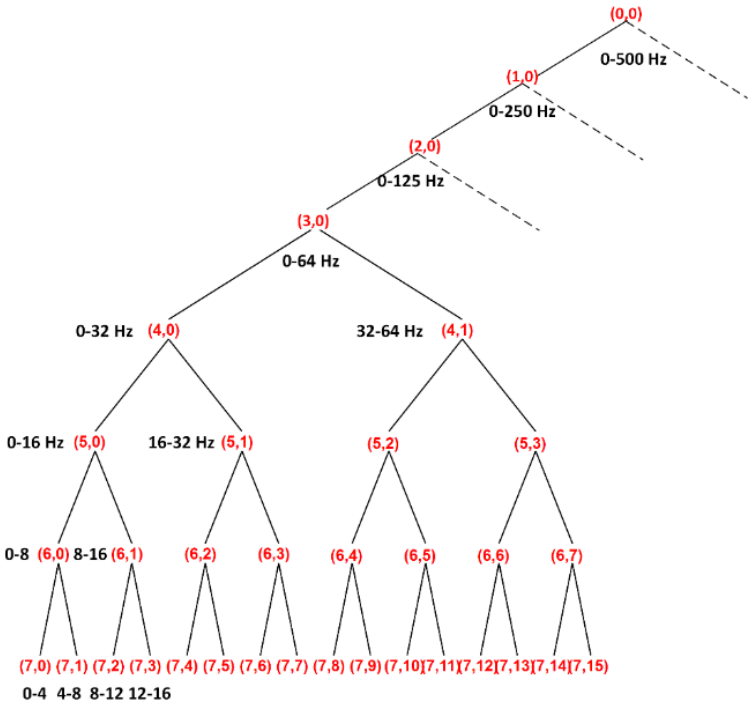

2.4. EEG Signal Data Extraction

Brain signals were recorded across 31 channels for each participant during 10 experimental stages: rest1, trial1, trial2, trial3, trial4, trial5, trial6, trial7, trial8, and rest2. The **rest1** signal represents the relaxation state before learning and memory formation, while **rest2** reflects the

relaxation state after learning and memory creation. The signals from **trial1 to trial8** correspond to the execution of the RAVLT task. Measurements of the Hurst exponent, Higuchi fractal dimension, approximate entropy, and sub-frequency bands (Delta, Theta, Alpha, Beta, and Gamma) were calculated for these signals using the methods detailed later in this article.

2.5. Higuchi Fractal Dimension:

One of the modern approaches for estimating complexity and exploring scale-free spaces in time series is fractal analysis. The Higuchi method for estimating the fractal dimension has gained significant attention from researchers due to its high accuracy and widespread application in EEG signal analysis, outperforming other methods such as box counting and Katz. However, it is more sensitive to noise compared to other fractal dimension estimation techniques (Wanliss & Wanliss, 2022).

2.6. Primary Processing of EEG Signals:

The primary signal analysis was conducted using MATLAB 2017 and SPSS software. This included estimating the Higuchi fractal dimension, the Hurst exponent, the approximate entropy of signals, and the relative power of sub-frequency bands (Equation 3). The statistical significance of these changes was validated using one-way ANOVA tests and the Bonferroni correction criterion.

$$Relative\ power = \frac{P_{sub\ band}}{P_{totla\ bands}} \qquad (3)$$

In the Higuchi fractal dimension calculation method, a new series is constructed from the input data series $x(1), x(2), \dots, x(N)$ as follows: For *m=1,2, 3 , … , k.*

$$x_m^k = \left\{x(m), x(m+k), x(m+2k), \dots\dots, x\left(m + \left\lfloor\frac{N-m}{k}\right\rfloor k\right)\right\} \qquad (4)$$

Here, *m* represents the starting point of each series, and ⌊ ⌋ represents the integer part of a number. For each x_m^k the length $L_m(k)$ is calculated as:

$$L_m(k) = \frac{\sum_{i=1}^{\left\lfloor\frac{N-m}{k}\right\rfloor} |x(m+ik) - x(m+(i-1)k)|}{\left\lfloor\frac{N-m}{k}\right\rfloor k} \quad N-1/k \qquad (5)$$

Here, N represents the total number of samples, and the normalization factor referenced in Equation (4) ensures consistency. For each value of k, the corresponding lengths $L_m(k)$ are computed, and their average is taken as the mean length. This process is repeated up to k_{max} . The Higuchi fractal dimension is then determined as the slope of the best-fit line, approximated using the least squares method, for $\log(L(k))$ versus $\log(k)$ (Vega & Noel, 2015).

In the calculation of the Higuchi fractal dimension, $k_{max} = 70$ is chosen, representing the maximum fractal dimension values within this time window. Beyond this point, the fractal dimension effectively stabilizes.

The fractal dimension and the Hurst exponent are related by the linear formula given in Equation (6):

$$D = 2 - H \qquad (6)$$

Here, D represents the fractal dimension, and H denotes the Hurst exponent.

For a completely random time series, the fractal dimension D equals 1.5. The fractal dimension values of EEG signals decrease as the memory content in the EEG signals increases, due to the rise in the Hurst exponent values, as described by Equation (6) (Vega & Noel, 2015).

3. Findings

The results of the Rey Auditory Verbal Learning Test (RAVLT) behavioral assessment show the average total number of words recalled across all participants, as depicted in Figure (5). With the progression of learning stages, the learning rate, or the number of words recalled by participants, demonstrates an upward trend. In stage t6, when the second list is introduced, the average RAVLT results for both genders, as shown in Figure (6), indicate that verbal and auditory learning and memory consolidation occur under relatively similar conditions for both males and females.

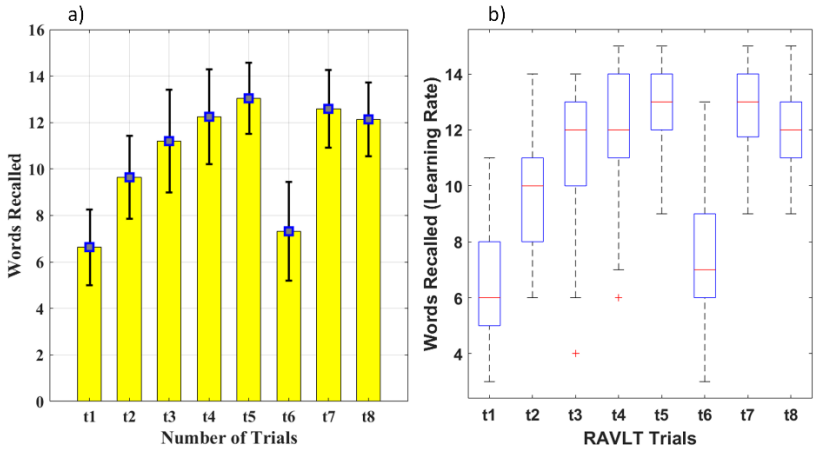

Figure 5 *Results of the RAVLT behavioral assessment of learning and memory consolidation across 8 stages.*

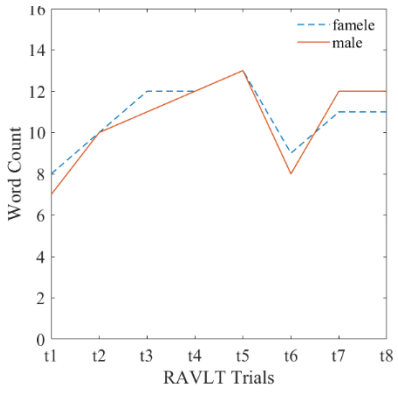

Figure 6 *Learning and memory consolidation trends in the RAVLT test for males and females*

All three variables extracted from the signals are displayed in Figure (7). As shown in part

(a) of the figure, the Higuchi fractal dimension of the EEG signals across all participants exhibits a strongly decreasing trend, with only a slight increase observed in stage t6 due to the presentation of the second list and its interference with the learning from the previous five stages.

In part (b), the changes in the Hurst exponent of the signals show an upward trend, indicating an increase in the memory capacity of the signals. Part (c) illustrates the changes in approximate entropy, confirming the findings of parts (a) and (b). It shows that a reduction in fractal dimension and an increase in the Hurst exponent correspond to a decline in random behavior. The decrease in approximate entropy, coupled with the increase in learning and memory consolidation rates, further supports this observation.

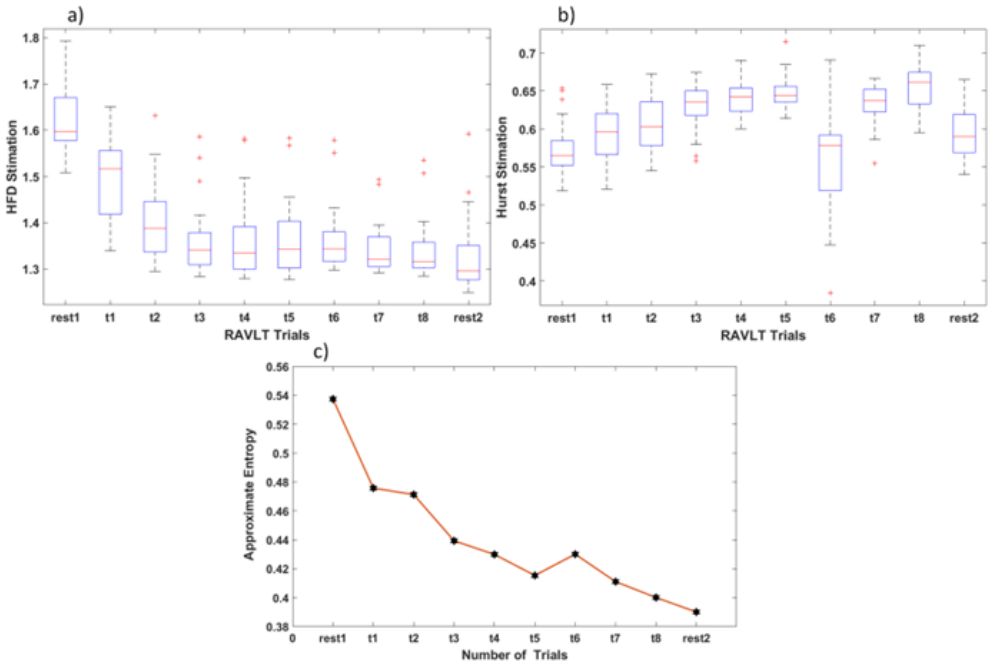

Figure 7 *Changes in information extracted from signals during learning and memory consolidation:(a) Box plot showing the decreasing trend of the Higuchi Fractal Dimension (HFD) of brain signals across all participants during the 10 stages of the RAVLT learning test. (b) Box plot depicting the increasing trend of the Hurst exponent of brain signals across all participants during the 10 stages of RAVLT learning and memory consolidation. (c) Decreasing trend of approximate entropy in brain signals during the learning and memory consolidation stages*

The **o**ne-way analysis of variance (ANOVA) table for the behavioral learning rate in the RAVLT test across 8 experimental stages. Table (2, 3, 4, 5) indicates that the changes in the Higuchi fractal dimension, Hurst exponent, and approximate entropy of the signals during the 10 recording stages are statistically significant, with a p-value << 0.01 confirming these changes.

Table 2 *One-way analysis of variance (ANOVA) for the behavioral learning rate in the **RAVLT** test across 8 experimental stages.*

Source	SS	df	MS	F	p-value
Between	277	7	39	11	0.0
	1.58		5.94	7.08	000

	Wit	**173**	**5**	**3.3**
hin	**1.42**	**12**	**82**	
	Tota	**450**	**5**	
l	**3**	**19**		

Table 3 *One-way analysis of variance (ANOVA) for changes in the Higuchi fractal dimension across 10 experimental stages*.

Source	SS	df	MS	F	p-value
Between	**2.36252**	**9**	**0.2625**	**51.17**	**0.0000**
Within	**1.53907**	**300**	**0.00513**		
Total	**3.90159**	**309**			

Table 4 *One-way analysis of variance (ANOVA) for changes in the Hurst exponent of signals across 10 experimental stages.*

Source	SS	df	MS	F	p-value
Between	**0.30505**	**9**	**0.03389**	**28.74**	**0.0000**
Within	**0.35378**	**300**	**0.00118**		
Total	**0.65883**	**309**			

Table 5 *One-way analysis of variance (ANOVA) for changes in approximate entropy across 10 experimental stages.*

Source	SS	df	MS	F	p-value
Between	**0.00079**	**9**	**0.0000088**	**37.65**	**0.0000**
Within	**0.0007**	**300**	**.00000023**		

Total	**0.00149**	**309**

To compare the effectiveness of the calculated variables, the effect size metric has been used. This statistic is calculated using the following equation:

$$\omega^2 \cong \frac{SSB}{SST} * 100 \quad (7)$$

ω2 represents the effect size, SSB denotes the sum of squares between groups, and SST refers to the total sum of squares, as introduced in Equation (8,9). μ represents the mean of each group, *n* is the total number of samples, *k* is the total number of groups, and *l* is the number of samples within each group. It is worth noting that these values can also be extracted from the first column of the one-way (ANOVA) table.

$$SST = \sum_{j=1}^{n} (x_j - \mu)^2 \quad (8)$$

$$SSB = \sum_{j=1}^{k} n_j (x_j - \mu)^2 \quad (9)$$

The results obtained from the frequency sub-bands related to the calculation of the Higuchi Fractal Dimension, as shown in Figure (8), indicate a decreasing trend in this variable across all stages. This reflects the integration of different brain regions during the progression of learning.

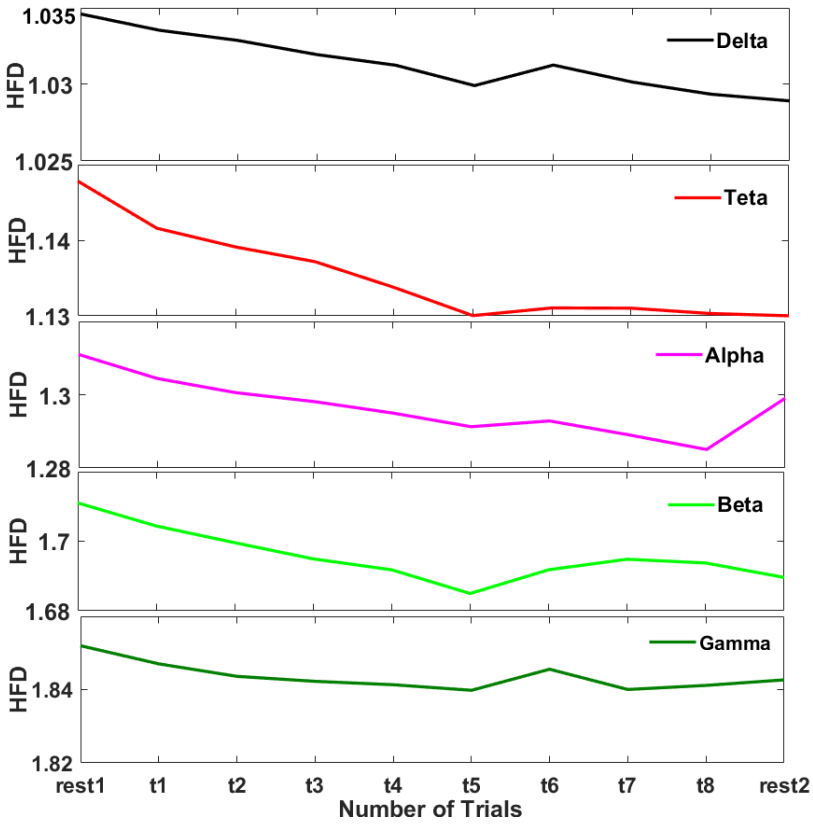

Figure 8 *The average Higuchi Fractal Dimension (HFD) across frequency bands from top to bottom, along with standard error: Delta, Theta, Alpha, Beta, and Gamma*.

In this study, to examine the correlation and relationship between variables, the variables were initially divided into two groups. The first group represents the dependent variable, which includes "WORD," referring to the number of words recalled in the RAVLT behavioral learning test. The second group consists of independent or predictor variables, including HURST as the Hurst exponent, HFD as the Higuchi Fractal Dimension, and ApEn as Approximate Entropy. The dependent variable, WORD, as defined in Equation (10), represents the mean difference in the number of words recalled during the RAVLT behavioral test across two stages, *trial5* and *trial1*, as well as the subtraction of *trial6* and the sum of *trial8*. This variable exhibits an upward trend across 65 subjects, with a decline observed during the sixth (interference) stage, followed by an increase in the eighth stage. The independent variables HFD, ApEn, and HURST were selected from the EEG recording channels that exhibited the most significant changes across all subjects. Using Equations (11), (12), and (13), the independent variables were defined and calculated for all subjects (65 samples). In Equation (11), the HURST variable demonstrates a positive trend, whereas in Equations (12) and (13), the ApEn and HFD variables show a negative and decreasing trend. All variables are defined with the subscript *diff*. The reason for using stages 1, 5, 6, and 8 for the independent variables is their impact on the learning and memory formation process, as can be clearly observed in Figure (7).

$$\mathrm{RAVLT}_{\mathrm{trial5}} - \mathrm{RAVLT}_{\mathrm{trial1}} + \mathrm{RAVLT}_{\mathrm{trial6}} - \mathrm{RAVLT}_{\mathrm{trial8}} = \mathrm{RAVLT}_{\mathrm{diff}} \quad (10)$$

$$\mathrm{HURST}_{\mathrm{trial5}} - \mathrm{HURST}_{\mathrm{trial1}} + \mathrm{HURST}_{\mathrm{trial6}} - \mathrm{HURST}_{\mathrm{trial8}} = \mathrm{HURST}_{\mathrm{diff}} \quad (11)$$

$$\mathrm{ApEn}_{\mathrm{trial5}} - \mathrm{ApEn}_{\mathrm{trial1}} + \mathrm{ApEn}_{\mathrm{trial6}} - \mathrm{ApEn}_{\mathrm{trial8}} = \mathrm{ApEn}_{\mathrm{diff}} \quad (12)$$

$$\mathrm{HFD}_{\mathrm{trial5}} - \mathrm{HFD}_{\mathrm{trial1}} + \mathrm{HFD}_{\mathrm{trial6}} - \mathrm{HFD}_{\mathrm{trial8}} = \mathrm{HFD}_{\mathrm{diff}} \quad (13)$$

3.1. Design of the Linear Regression Model

Statistical modeling is an effective method for analyzing data and estimating the linear relationship between independent or predictor variables and the dependent variable. However, this relationship may not always be linear, potentially requiring curve fitting or polynomial modeling. In either case, the goal is to design a simple linear or curved model that passes through the majority of data points, minimizing the distance between the data points and the fitted line or regression error. To enhance the accuracy and efficiency of the model, in this study, the variables were calculated with high precision using advanced mathematical methods to establish the necessary relationships in the model appropriately.

3.2. The statistical regression model for the Hurst exponent, Higuchi Fractal Dimension, and Approximate Entropy of EEG signals aims to estimate the behavioral learning rate (WORD).

In this study, to examine the relationship between the dependent and independent variables, a scatter plot of these variables was created, as shown in Figure (9).

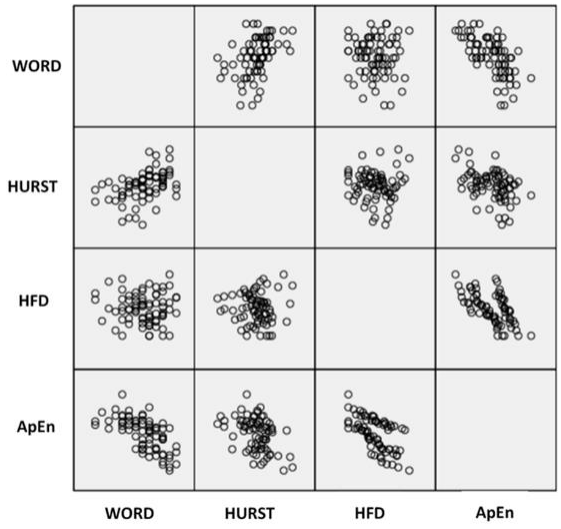

Figure 9 *Scatter plot between the variables WORD (number of words recalled), HURST (Hurst exponent of the signals), HFD (Higuchi Fractal Dimension of the signals), and ApEn (Approximate Entropy of the signals).*

According to the summary model table (Table 6), the adjusted coefficient of determination is 0.704, the correlation coefficient is 0.846, and the coefficient of determination is 0.716. The capability of this regression model to statistically estimate the dependent variable (behavioral learning rate) based on the quantities extracted from the signals is satisfactory. The analysis of variance tables (Tables 2, 3, and 4), with p-value<<0.05, also confirm the adequacy of the designed model.

Table 6 *Summary table of the model for the dependent variable WORD in relation to the independent variables HURST, HFD, and ApEn.*

Model	R	R Square	Adjusted R Square	Std. Error of the Estimate
1	.846[a]	.716	.704	1.54301

To determine the regression model coefficients, the coefficient table in SPSS software was utilized, and the model is presented based on Equation (14). The calculated regression model demonstrates the relationship between the behavioral learning rate and the Hurst exponent, Higuchi Fractal Dimension, and Approximate Entropy. According to this model, the most significant independent variable is the Higuchi Fractal Dimension of the signals. In the final stage, to assess the regression model's error, an evaluation was conducted as outlined. The results of this evaluation indicate that the designed model can predict the behavioral learning rate with an accuracy of 78.33%.

$$WORD = 2878{,}486 - 45{,}845 * HURST - 2785{,}662 * HFD - 112{,}24 \quad (14)$$

The decreasing trend in the Higuchi Fractal Dimension (HFD) with the progression of learning stages—before learning (rest1) and during learning (trial1 to trial5)—across all frequency sub-bands $\gamma, \beta, \alpha, \theta, \delta$ is clearly observed in Figure (8). However, in the seventh signal recording stage (t6), the frequency sub-bands exhibit a sudden upward change due to the introduction of the new word list "B" and its interference with current and previous memory formation. In stages t7 and t8, where the "A" word list is reintroduced, the trend is expected to return to its prior decreasing trajectory due to reliance on earlier memories, though the alpha and gamma sub-bands do not follow this pattern.

The largest effect size of fractal dimension changes occurs in the lower frequency theta band at 70.78% and in the higher frequency beta band at 65.44%. Notably, across all sub-bands, the fractal dimension after learning (rest2) shows a decrease compared to the pre-learning stage (rest1).

3.3. Regression Model for Frequency Sub-Bands to Predict Behavioral Learning Rate (Variable WORD)

The human brain, as an example of a complex system, consists of components that play a crucial role in organizing cognitive behaviors. One of the most important elements enabling information processing in the brain across various temporal and spatial scales is the frequency sub-bands that constitute brain signals. In this study, one of the objectives of modeling brain behavior is to utilize these sub-bands in predicting the learning rates of subjects.

As observed in the regression model (Equation 14), the most suitable variable (largest

coefficient in the model) for predicting the behavioral learning rate is the Higuchi Fractal Dimension. This measure was also utilized in this stage of statistical modeling within the frequency sub-bands.

As in the previous stage, the condition for using parametric statistical tests (normal distribution), such as analysis of variance, paired t-tests, and curve fitting, is the normal distribution of the variable under study. The Kolmogorov-Smirnov test was used to evaluate the normality of the HFD variable across frequency sub-bands, and the results of this test, along with histograms of the variables. As shown in this table, the Higuchi Fractal Dimension across all frequency sub-bands has p-value>0.05, and the null hypothesis (H_0)is confirmed, indicating that the HFD variable follows a normal distribution in all sub-bands.

The first step in examining the relationship between the variables is to use a scatter plot of the Higuchi Fractal Dimension of the frequency sub-bands (independent variable) against the number of words recalled (dependent variable), as shown in Figure (10).

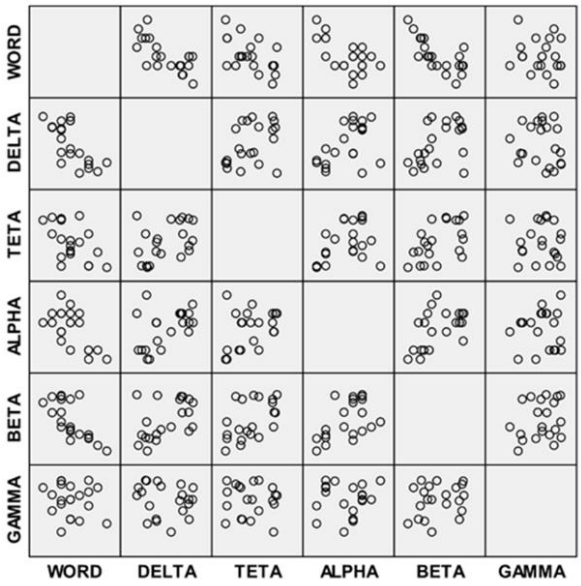

Figure 10 *Scatter plot of the dependent variable **WORD** (number of words recalled) against the Higuchi Fractal Dimension of the frequency sub-bands: Delta, Theta, Alpha, Beta, and Gamma (independent variables).*

To define the fitting model between the response variable and other variables, which include all sub-bands with pvalue << 0.05 impacting the model, Equation (15) is used. Only the constant term does not meet the required conditions and is therefore not included in the regression model described by Equation (15).

$$WORD = -330{,}212 * DELTA - 349 * TETA - 19{,}81 * ALPHA - 146{,}42 * BETA \ - 91{,}55 * GAMMA \qquad (15)$$

As observed in the regression model (Equation 15), the impact of each sub-band on the learning variable (WORD) is decreasing. This is attributed to the declining trend of the Higuchi Fractal

Dimension during the learning process. These changes align with previous studies (Klonowski; Leahey; Soria-Frisch, 2004; Wixted & Thompson-Schill, 2018), confirming the significant role of the Theta band in successive cognitive processes, such as the RAVLT learning test, where the subject must follow a series of repeated words over multiple stages. Changes in the Beta band also have a substantial effect on recall during memory formation processes.

The multiple statistical modeling in this study, as shown in Equation (14), demonstrates a significant linear relationship (correlation coefficient R=0.846) between the behavioral learning rate assessed in the RAVLT test and the nonlinear parameters of the Hurst exponent, Higuchi Fractal Dimension, and Approximate Entropy of the signals. As the subject focuses on recall and increases memory content, a simultaneous increase in memory and a decrease in entropy are observed in the brain signals. The contribution of the Higuchi Fractal Dimension (HFD) of brain signals in this model is clearly evident. The accuracy of this model, based on the model evaluation table, is 78.33%.

In the second model developed in this study, the relationship between the Higuchi fractal dimension of sub-frequency bands as predictor variables and the behavioral learning rate was designed according to Equation (10). The correlation coefficient (R=0.865) in this statistical regression model indicates its strong efficiency, with an accuracy of 73.27%. This model predicts the RAVLT behavioral learning rate based on changes in the Higuchi fractal dimension of the sub-frequency bands.

The model clearly demonstrates the role of the theta band at low frequencies and the beta band at high frequencies. As observed in the memory processes (encoding, consolidation, and recall) in this study, the theta band shows the highest Higuchi fractal dimension during information recall, while the beta band exhibits the highest Higuchi fractal dimension during information encoding. These findings are consistent with previous research (Atkinson & Shiffrin, 1968; Loftus & Loftus, 2019; Rahmani et al., 2018).

The results of this study confirm the role of the theta band in synchronizing connections between brain regions and enhancing working memory activity for memory formation. Similarly, the beta band is shown to increase conscious performance and brain attention.

3.4. Results of the Hurst Exponent and Fractal Dimension of Signals in Relation to the RAVLT Test

This section examines the relationship between RAVLT behavioral learning and the mathematical index of the Hurst exponent in signals. As shown in part (a) of Figure (5), the values of the Hurst exponent increase with the rising number of words recalled by the participant. This positive correlation aligns with a previous study (Gottlieb, 2012), where the increase in memory signals was confirmed only for sensory memory over brief moments. This finding indicates that as memory formation processes intensify in the brain cortex, the Hurst exponent of the signals also rises, representing an increase in memory within the signals. In other words, what is evaluated behaviorally is also confirmed in brain signals.

The relationship described in Equation (6), where the sum of the fractal dimension and the Hurst exponent equals a random variable with a value of 2, is validated in part (b) of Figure (11). A detailed analysis of the changes in signal indices, such as the Higuchi fractal dimension and the Hurst exponent at each stage of the learning process, is a key advantage of this study. It

enables more precise monitoring of learning dynamics.

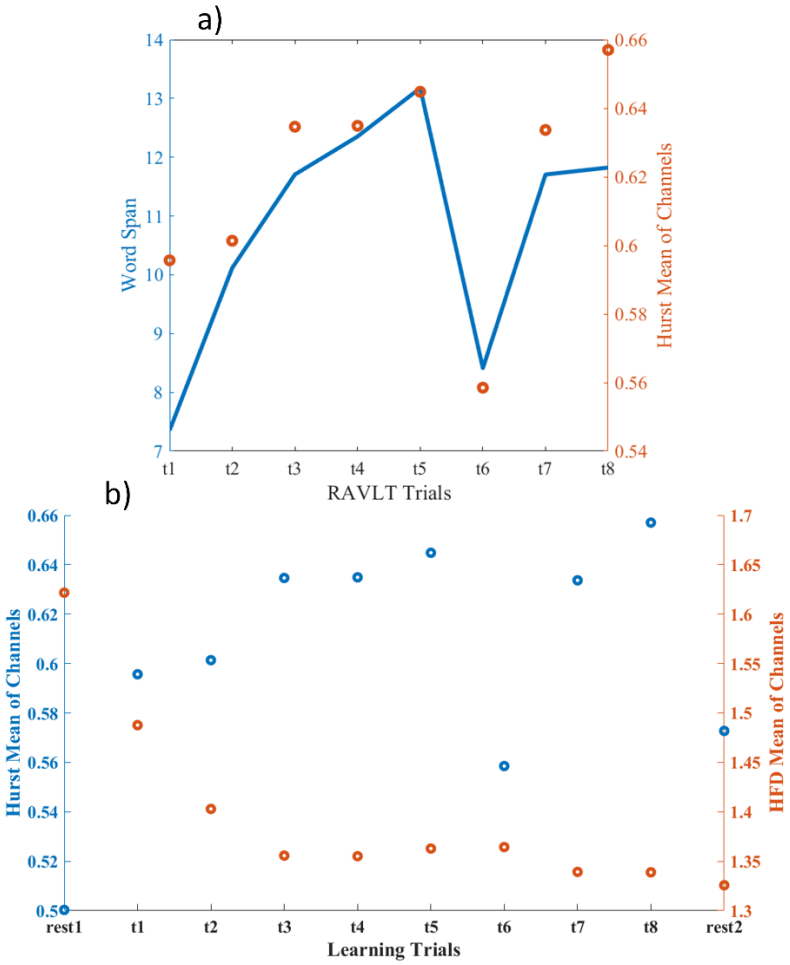

Figure 11 *Relationship between variables extracted from signals:*
(a) Simultaneous changes in the average Higuchi fractal dimension with the increasing behavioral learning rate in RAVLT. (b) Correlation between changes in the fractal dimension (blue) and the Hurst exponent (red circles), approximating the relationship D=2−H.

Discussion

In the RAVLT behavioral test, the participants demonstrated two stages of performance during the memory formation process, as shown in Figure (12). The first stage, lasting 15 seconds, involved presenting the words to the participants, during which they were required only to listen. According to the memory formation theory, in this stage, the input information is encoded and stabilized through auditory and verbal pathways. In the second stage, participants were given 45 seconds to recall the memorized words and articulate them based on their verbal memory. The correct articulation of each word, for instance, is considered a behavioral score and ultimately contributes to the participant's increased learning rate.

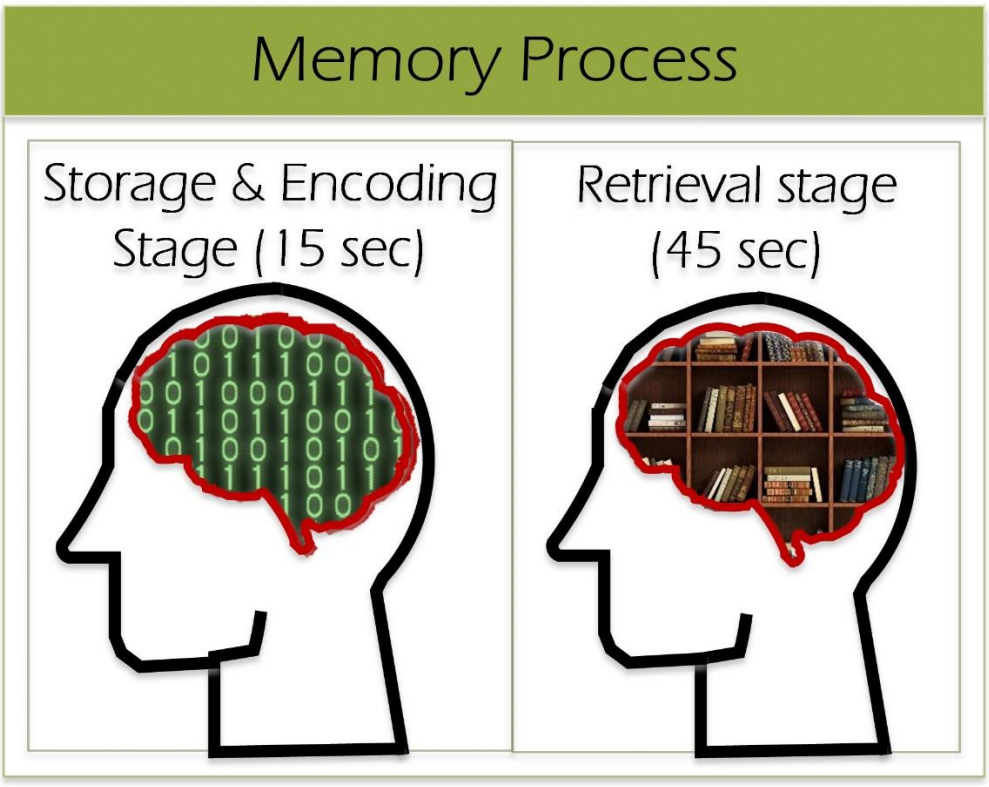

Figure 12 *Illustration of memory processes in the RAVLT behavioral learning test, comprising two phases: Encoding and stabilization of information Recall of information*

In this study, as shown in Figure (13), there is little difference in power spectral density between the encoding-stabilization phase and the word recall phase. As observed in part (a) of this figure, the power of these two phases shows minimal difference at the beginning of the learning process (trial1). However, with the progression of learning and memory formation, by the final stage (trial8), the power spectral density of signals during the recall phase is significantly lower than during the encoding phase. This indicates better stabilization and structuring of memory in the final stage of behavioral learning. Additionally, the reduction in recall-phase power in trial8 reflects the participant's mastery and enhanced organization of information in memory.

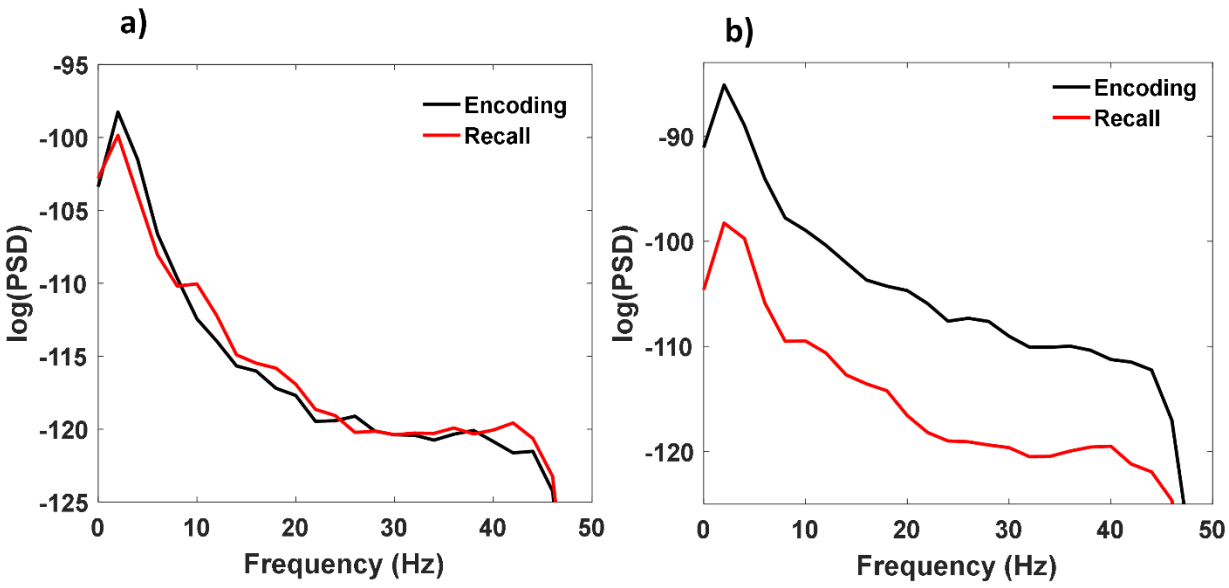

Figure 13 *Comparison of power spectral density in the two phases: encoding and stabilization (red curve) and recall (black curve): (a) During the first learning stage (trial1) (b) During the final learning stage (trial8)*

In the brain mapping derived from dynamic brain activity, the distribution of the Higuchi fractal dimension of signals during trial1 and trial8 is compared in the encoding and recall phases, as shown in Figure (14). As observed, the distribution of the Higuchi fractal dimension in the recall phase during trial8 is significantly lower than during trial1. This reduction reflects a decrease in the brain's fractal behavior due to the increased learning rate and enhanced coordination among various brain regions in trial8.

Another noteworthy observation is that the dynamic activity of the right hemisphere is greater than that of the left hemisphere in both encoding and recall phases (Gottlieb, 2012; Rahmani et al., 2018). The results of the paired t-test for the Higuchi fractal dimension of sub-frequency bands, align with previous studies, demonstrating the influence of the theta sub-frequency band during both encoding and recall phases, and the impact of the beta band during recall (Bjork & Bjork, 1996; Kristoufek & Vosvrda, 2014).

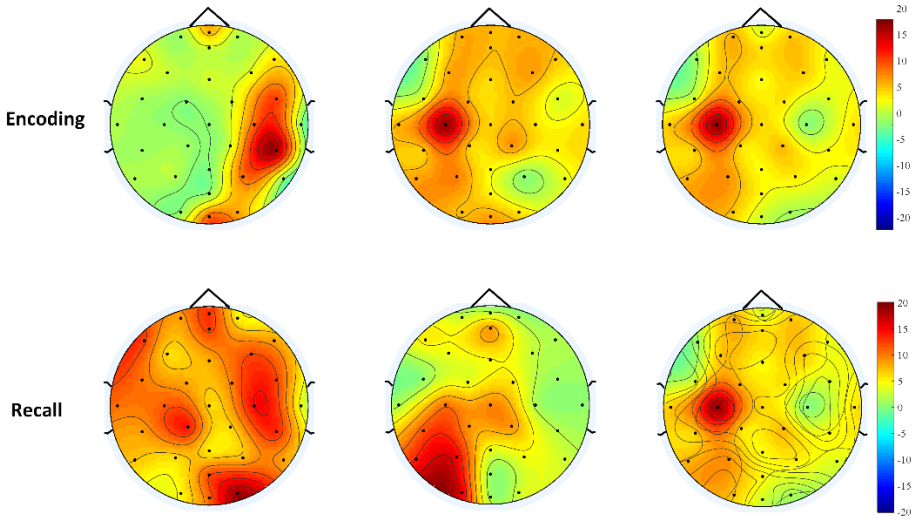

Figure 14 *Comparison of brain maps showing the distribution of the Higuchi fractal dimension in the encoding and recall phases during the first learning stage (trial1) and the final learning stage (trial8).*

Future objectives of this research could involve using healthy subjects and individuals with ADHD or groups with learning disorders for comparative studies. This would include evaluating the results of the RAVLT behavioral test alongside the extracted signal data and the chaotic behavior of the signals.

4. Conclusion

The multivariate statistical modeling in this study, as presented in Equation (14), demonstrates a significant linear relationship (correlation coefficient R=0.846) between the behavioral learning rate assessed via the RAVLT and the nonlinear parameters of the Hurst exponent, Higuchi fractal dimension (HFD), and approximate entropy of the signals.

As the participant focuses on recalling and increasing memory content, a simultaneous increase in memory and decrease in entropy are observed in the brain signals. The contribution of the Higuchi fractal dimension (HFD) of brain signals is prominently evident in this model. The model's accuracy, is reported as 78.33%.

In the second model designed in this study, the Higuchi fractal dimension (HFD) of frequency sub-bands was used as predictive variables to estimate the behavioral learning rate, as described in Equation (15). The correlation coefficient (R = 0.865) in this statistical regression model indicates its efficiency, with an accuracy of 73.27%.

This model effectively predicts the RAVLT behavioral learning rate by analyzing the changes in the HFD of sub-bands. It highlights the role of the theta band at lower frequencies and the beta band at higher frequencies. Results show that the theta band exhibits the highest HFD value during the recall phase, while the beta band demonstrates the highest HFD value during

the encoding phase of information. These findings align with previous studies (Bjork & Bjork, 1996; Ceballos & Largo, 2018; Cowan, 2005; Wixted & Thompson-Schill, 2018).

The study also confirms that the activity of the theta band plays a crucial role in coordinating brain regions and enhancing working memory to facilitate memory formation. Similarly, the activity of the beta band is associated with increased conscious and attentive brain performance.

Acknowledgment:
This research is derived from a section of a doctoral dissertation, conducted in collaboration with the Arak University of Technology for signal recording from subjects and the Cognitive Science Faculty of Shahid Beheshti University for scientific consultation.

References

Aben, B., Stapert, S., & Blokland, A. (2012). About the distinction between working memory and short-term memory. *Frontiers in psychology*, *3*, 301. https://doi.org/10.3389/fpsyg.2012.00301

Alsaeed, N. H. (2017). Wish you were here: A psychological analysis using Atkinson-Shiffrin memory mode. *Journal of Literature and Art Studies*, *6*(5), 521-527. https://doi.org/10.17265/2159-5836/2017.05.004

Amin, H. U., & Malik, A. S. (2014). Memory retention and recall process. *EEG/ERP analysis: Methods and applications*, 219-237. https://doi.org/10.1201/b17605-11

Amina, H. U., & Malikb, A. S. (2019). Learning and Memory Improvement: Evidence from Current Research and Neurofeedback Applications. *Asia Pacific Journal of Neurotherapy*, *1*(2), 1-9.

Antonis, T. (2023). The Basic Cognitive Functions. *Anna Clin Rev Cas Rep: ACRCR-115*. https://doi.org/10.47991/ACRCR/2837-3642/100115

Arab, M. R., Setoudeh, F., Khosroabadi, R., Najafi, M., & Tavakoli, M. B. (2022). EEG signal processing for survey of dynamic auditory verbal learning and memory formation in brain by fractal analysis. *Fluctuation and Noise Letters*, *21*(01), 2250010. https://doi.org/10.1142/S0219477522500109

Atkinson, R. C., & Shiffrin, R. M. (1968). Human memory: A proposed system and its control processes. In *Psychology of learning and motivation* (Vol. 2, pp. 89-195). Elsevier. https://doi.org/10.1016/S0079-7421(08)60422-3

Baars, B. J., & Gage, N. M. (2010). *Cognition, brain, and consciousness: Introduction to cognitive neuroscience*. Academic Press.

Baddeley, A. (2006). Working memory: An overview. *Working memory and education*, 1-31.

Basar, E. (2004). *Memory and brain dynamics: Oscillations integrating attention, perception, learning, and memory*. CRC press. https://doi.org/10.1201/9780203298732

Benedek, M., & Fink, A. (2019). Toward a neurocognitive framework of creative cognition: The role of memory, attention, and cognitive control. *Current Opinion in Behavioral Sciences*, *27*, 116-122. https://doi.org/10.1016/j.cobeha.2018.11.002

Birbaumer, N., & Cohen, L. G. (2007). Brain–computer interfaces: communication and restoration of movement in paralysis. *The Journal of physiology*, *579*(3), 621-636. https://doi.org/10.1113/jphysiol.2006.125633

Bjork, E. L., & Bjork, R. A. (1996). *Memory*. Elsevier.

Bongers, A., Flynn, A. B., & Northoff, G. (2020). Is learning scale-free? Chemistry learning increases EEG fractal power and changes the power law exponent. *Neuroscience Research*, *156*, 165-177. https://doi.org/10.1016/j.neures.2019.10.011

Brem, A.-K., Ran, K., & Pascual-Leone, A. (2013). Learning and memory. *Handbook of clinical neurology*, *116*, 693-737. https://doi.org/10.1016/B978-0-444-53497-2.00055-3

Brown, R., Brown, R. E., & Brown, R. E. (1994). *An introduction to neuroendocrinology*. Cambridge University Press.

Bullmore, E. T., & Bassett, D. S. (2011). Brain graphs: graphical models of the human brain connectome. *Annual review of clinical psychology*, *7*(1), 113-140. https://doi.org/10.1146/annurev-clinpsy-040510-143934

Ceballos, R. F., & Largo, F. F. (2018). On the estimation of the Hurst exponent using adjusted rescaled range analysis, detrended fluctuation analysis and variance time plot: A case of exponential distribution. *arXiv preprint arXiv:1805.08931*. https://doi.org/10.48550/arXiv.1805.08931

Ceglarek, A., Ochab, J. K., Cifre, I., Fafrowicz, M., Sikora-Wachowicz, B., Lewandowska, K.,…Chialvo, D. R. (2021). Non-linear functional brain co-activations in short-term memory distortion tasks. *Frontiers in Neuroscience*, *15*, 778242. https://doi.org/10.3389/fnins.2021.778242

Cowan, N. (2005). Working memory capacity limits in a theoretical context. Human learning and memory: Advances in theory and application. The 4th Tsukuba international conference on memory,

Crowder, R. G. (2014). *Principles of learning and memory: Classic edition*. Psychology Press.

Daryadar, M., & Raghibi, M. (2015). The effect of listening to recordings of one's voice on attentional bias and auditory verbal learning. *International Journal of Psychological Studies*, *7*(2), 155. https://doi.org/10.5539/ijps.v7n2p155

Davis, C. E., Hauf, J. D., Wu, D. Q., & Everhart, D. E. (2011). Brain function with complex decision making using electroencephalography. *International journal of psychophysiology*, *79*(2), 175-183. https://doi.org/10.1016/j.ijpsycho.2010.10.004

Dubinsky, J. M., & Hamid, A. A. (2024). The Neuroscience of Active Learning and Direct Instruction. *Neuroscience & Biobehavioral Reviews*, 105737. https://doi.org/10.1016/j.neubiorev.2024.105737

Fard, E. K., Keelor, J. L., Bagheban, A. A., & Keith, R. W. (2016). Comparison of the Rey Auditory Verbal Learning Test (RAVLT) and digit test among typically achieving and gifted students. *Iranian Journal of Child Neurology*, *10*(2), 26.

Feng, Z., He, Q., Zhang, J., Wang, L., Zhu, X., & Qiu, M. (2020). A hybrid BCI system based on motor imagery and transient visual evoked potential. *Multimedia Tools and Applications*, *79*(15), 10327-10340. https://doi.org/10.1007/s11042-019-7607-3

Geake, J. (2009). *The brain at school: Educational neuroscience in the classroom: Educational neuroscience in the classroom*. McGraw-Hill Education (UK).

Gneiting, T., & Schlather, M. (2004). Stochastic models that separate fractal dimension and the Hurst effect. *SIAM review*, *46*(2), 269-282. https://doi.org/10.48550/arXiv.physics/0109031

Gottlieb, J. (2012). Attention, learning, and the value of information. *Neuron*, *76*(2), 281-295. https://doi.org/10.1016/j.neuron.2012.09.034

Kaufmann, T., Herweg, A., & Kübler, A. (2014). Toward brain-computer interface based wheelchair control utilizing tactually-evoked event-related potentials. *Journal of neuroengineering and rehabilitation*, *11*, 1-17. https://doi.org/10.1186/1743-0003-11-7

Klonowski, W. (2016). Fractal analysis of electroencephalographic time series (EEG Signals). *The fractal geometry of the brain*, 413-429. https://doi.org/10.1007/978-1-4939-3995-4_2

Ko, L.-W., Ranga, S., Komarov, O., & Chen, C.-C. (2017). Development of Single-Channel Hybrid BCI System Using Motor Imagery and SSVEP. *Journal of healthcare engineering*, *2017*(1), 3789386. https://doi.org/10.1155/2017/3789386

Kristoufek, L., & Vosvrda, M. (2014). Measuring capital market efficiency: long-term memory, fractal dimension and approximate entropy. *The European Physical Journal B*, *87*(7), 162. https://doi.org/10.1140/epjb/e2014-50113-6

Leahey, T. H. Fundamentals of Cognitive Science: Minds, brain, magic, and evolution.

Loftus, G. R., & Loftus, E. F. (2019). *Human memory: The processing of information*. Psychology Press. https://doi.org/10.4324/9781315787145

Maye, A., Zhang, D., Wang, Y., Gao, S., & Engel, A. K. (2011). Multimodal brain-computer interfaces. *Tsinghua Science and Technology*, *16*(2), 133-139. https://doi.org/ 10.1016/S1007-0214(11)70020-7

Michel, C. M., & Brunet, D. (2019). EEG source imaging: a practical review of the analysis steps. *Frontiers in neurology*, *10*, 325. https://doi.org/10.3389/fneur.2019.00325

Miller, C. (2020). 8.7 Human Senses. *Human Biology*.

Mitchell, J. D., & Borasio, G. D. (2007). Amyotrophic lateral sclerosis. *The lancet*, *369*(9578), 2031-2041. https://doi.org/ 10.1016/S1007-0214(11)70020-7

Rahmani, B., Wong, C. K., Norouzzadeh, P., Bodurka, J., & McKinney, B. (2018). Dynamical Hurst analysis identifies EEG channel differences between PTSD and healthy controls. *PloS one*, *13*(7), e0199144. https://doi.org/10.1371/journal.pone.0199144

Ricci, M., Graef, S., Blundo, C., & Miller, L. A. (2012). Using the Rey Auditory Verbal Learning Test (RAVLT) to differentiate Alzheimer's dementia and behavioural variant fronto-temporal dementia. *The Clinical Neuropsychologist*, *26*(6), 926-941. https://doi.org/10.1080/13854046.2012.704073

Skeel, R. L., & Edwards, S. (2011). The assessment and rehabilitation of memory impairments. In *Rehabilitation of neuropsychological disorders* (pp. 47-73). Psychology Press.

Soria-Frisch, A. (2004). *Soft data fusion for computer vision*. Fraunhofer-IRB-Verlag. https://doi.org/10.13140/2.1.2701.2483

Sulak, S. A., & Koklu, N. (2024). Analysis of Depression, Anxiety, Stress Scale (DASS-42) With Methods of Data Mining. *European Journal of Education*, *59*(4), e12778. https://doi.org/10.1111/ejed.12778

Vega, C. F., & Noel, J. (2015). Parameters analyzed of Higuchi's fractal dimension for EEG brain signals. 2015 Signal Processing Symposium (SPSympo), https://doi.org/10.1109/SPS.2015.7168285

Wang, Z., Yu, Y., Xu, M., Liu, Y., Yin, E., & Zhou, Z. (2019). Towards a hybrid BCI gaming paradigm based on motor imagery and SSVEP. *International Journal of Human–Computer Interaction*, *35*(3), 197-205. https://doi.org/10.1080/10447318.2018.1445068

Wanliss, J., & Wanliss, G. E. (2022). Efficient calculation of fractal properties via the Higuchi method. *Nonlinear Dynamics*, *109*(4), 2893-2904. https://doi.org/10.1007/s11071-022-07353-2

Wixted, J. T., & Thompson-Schill, S. L. (2018). *Stevens' Handbook of Experimental Psychology and Cognitive Neuroscience, Language and Thought* (Vol. 3). John Wiley & Sons.